

Oxygen Permeation of a Dense/Porous Asymmetric Membrane Using $\text{La}_{0.6}\text{Ca}_{0.4}\text{CoO}_{3-\delta}$ – $\text{BaFe}_{0.975}\text{Zr}_{0.025}\text{O}_{3-\delta}$ System

Ken Watanabe,¹ Masayoshi Yuasa,² Tetsuya Kida,² Kengo Shimanoe,^{*2} Yasutake Teraoka,² and Noboru Yamazoe²

¹Department of Molecular and Material Sciences, Interdisciplinary Graduate School of Engineering Science, Kyushu University, 6-1 Kasuga-Koen, Kasuga 816-8580

²Department of Energy and Material Sciences, Faculty of Engineering Science, Kyushu University, 6-1 Kasuga-Koen, Kasuga 816-8580

(Received October 22, 2008; CL-081015; E-mail: shimanoe@mm.kyushu-u.ac.jp)

To achieve a high oxygen permeation rate at medium and high temperature, an asymmetrically structured membrane, in which a thin dense layer ($30\ \mu\text{m}$) made of $\text{La}_{0.6}\text{Ca}_{0.4}\text{CoO}_{3-\delta}$ (LCC) and $\text{BaFe}_{0.975}\text{Zr}_{0.025}\text{O}_{3-\delta}$ (BFZ) was formed on a porous LCC support, was fabricated and tested for its oxygen permeability. The oxygen permeation flux significantly increased by mixing BFZ with LCC and reached a fairly high value of $1.60\ \text{cm}^3\ \text{min}^{-1}\ \text{cm}^{-2}$ even at $780\ ^\circ\text{C}$.

Since Teraoka et al. reported that La–Sr–Co–Fe-based perovskite-type oxides show oxygen permeation properties at elevated temperature such as $900\ ^\circ\text{C}$ in 1985,¹ a number of Co-based perovskite-type oxides with high oxygen permeabilities have been developed.^{2,3} However, it is necessary to further improve the oxygen permeability for practical oxygen separation from air; oxygen permeation fluxes of more than $10\ \text{cm}^3$ (STP) $\text{min}^{-1}\ \text{cm}^{-2}$ are required for commercial uses.⁴ There are several reports of improving oxygen permeability; for example, composition control, surface modification, and structural optimization of membranes have been carried out. In particular, reduction of membrane thickness is an effective method of improving oxygen permeation because the oxide-ion diffusion distance can be decreased by decreasing the thickness. However, the fabrication of thin membranes with micrometer-order thickness is a challenge because of its low mechanical strength. In order to solve this problem, an asymmetric structure in which a dense layer is fabricated on a porous support was proposed as shown in Figure 1.⁵ Recently, we have reported that a $\text{La}_{0.6}\text{Ca}_{0.4}\text{CoO}_{3-\delta}$ (LCC)-based asymmetric membrane with a $10\ \mu\text{m}$ dense layer shows a remarkably improved oxygen permeation rate, as compared with that of a conventional sintered-disk-type LCC membrane,⁶ demonstrating a feasible way of upgrading membrane performance.

However, the oxygen permeation rate is still lower than required for practical application. In addition, an improvement in

the oxygen permeation rate particularly at temperatures around 700 – $800\ ^\circ\text{C}$ is necessary from the view point of energy saving in factories. Previously, we have reported that $\text{BaFe}_{0.975}\text{Zr}_{0.025}\text{O}_{3-\delta}$ (BFZ)-based sintered-disk-type membranes show higher oxygen permeation fluxes at medium and high temperature than that of LCC.⁷ Thus, it is expected that deposition of a thin BFZ layer on a porous LCC support would achieve an increase in the oxygen permeability. However, it is difficult to fabricate a dense BFZ layer on a porous LCC support because of the difference in the thermal expansion coefficients. In this study, to relax the difference in the thermal expansion coefficients, we tried to deposit a mixed LCC–BFZ layer on a porous LCC support and investigated the oxygen permeation properties of the asymmetric LCC–BFZ membrane.

A LCC porous support was fabricated by an oxalate method as described elsewhere.⁸ A mixed metal (La, Ca, and Co) nitrate solution was added to oxalic acid to form precursor precipitates, which were then dried at $120\ ^\circ\text{C}$ and calcined at $400\ ^\circ\text{C}$ in air. The calcined powder was press-formed into a disk to form a green porous support. A LCC powder for the dense layer was prepared by an amorphous malic acid precursor method.⁹ BFZ powder was prepared by pyrolysis of constituting metal nitrates and acetates.⁷ The LCC and BFZ powders were mixed in a weight ratio of LCC/BFZ = 4/1. This mixed powder was dispersed in ethanol to form a slurry (10 wt %). A portion (0.3 mL) of the slurry was coated on the porous green LCC support and dried at room temperature for a few hours. The slurry-coated membrane was sintered at $1150\ ^\circ\text{C}$ for 5 h in air to obtain the asymmetric LCC–BFZ membrane. No physical gas permeation was detected for the fabricated asymmetric membrane. The oxygen permeation test of the fabricated membranes was carried out in a gas flow apparatus using synthetic air ($200\ \text{mL}\ \text{min}^{-1}$) and He ($150\ \text{mL}\ \text{min}^{-1}$) as feed and sweep gases, respectively, as described elsewhere.⁶ The amount of oxygen permeated through the membrane was determined by a gas chromatography.

Figure 2 shows the XRD patterns of LCC, BFZ, and LCC–BFZ samples sintered at $1150\ ^\circ\text{C}$. The crystal structures of all samples can be ascribed to perovskite structure. The lattice constants of LCC, LCC–BFZ, and BFZ were determined to be 3.8, 4.0, and 4.1 Å respectively. Notably, the lattice constant of LCC–BFZ was different from those of the starting LCC and BFZ, indicating that LCC and BFZ formed a solid solution during high-temperature sintering, although the precise composition ratio was not determined. Figure 3 shows the surface and cross-sectional SEM photographs of the obtained asymmetric membrane. As seen in Figure 3a, there are no pores on the surface of the dense layer. The dense morphology of the LCC–BFZ layer

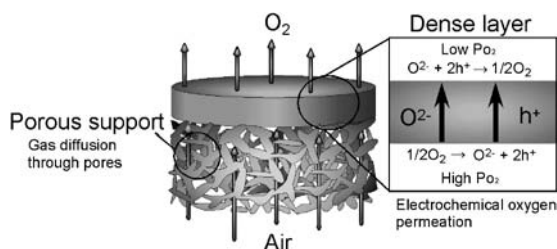


Figure 1. Schematic drawing of the dense/porous asymmetric membrane for oxygen separation using the mixed conductor.

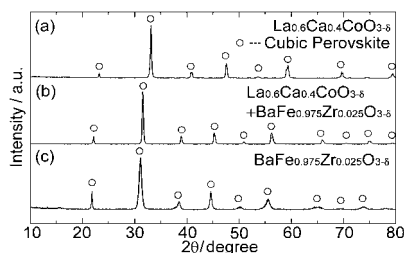


Figure 2. XRD patterns of powder samples sintered at 1150 °C: (a) LCC, (b) LCC/BFZ, and (c) BFZ.

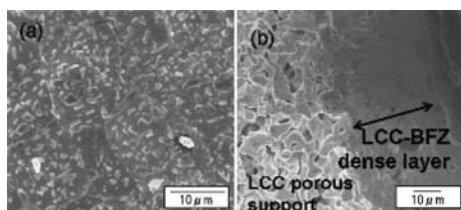


Figure 3. SEM photographs of (a) surface and (b) cross section of the fabricated asymmetric LCC–BFZ (4:1) membrane.

with about 30 μm thickness is also confirmed in Figure 3b. However, crack-free dense layers could not be obtained when the LCC/BFZ ratio was smaller than 4/1, for example, 3/1, 1/1, and 1/2. This seems to result from an increased difference in the thermal expansion coefficient between a LCC–BFZ layer and the porous LCC support particularly when the BFZ content is high.

Figure 4 shows the oxygen permeation flux of the asymmetric LCC–BFZ membrane as a function of temperature. For comparison, permeation fluxes of sintered-disk-type BFZ (1000 μm), asymmetric LCC (20 μm), and sintered-disk-type LCC (1200 μm) membranes were also plotted. Remarkably, the oxygen permeation flux of the asymmetric LCC–BFZ membrane was higher than that of the asymmetric LCC membrane at all operating temperatures and reached a high value of 3.65 cm^3 (STP) $\text{min}^{-1} \text{cm}^{-2}$ at 930 °C. The oxygen permeation flux would be further improved by forming a porous catalyst layer on the surface of the thin dense layer. Moreover, even at 780 °C, the oxygen permeation flux exceeded 1.6 cm^3 (STP) $\text{min}^{-1} \text{cm}^{-2}$. This value is much larger than that for other asymmetric membranes; for example, Araki et al. reported an oxygen permeation flux of about 0.6 cm^3 (STP) $\text{min}^{-1} \text{cm}^{-2}$ at 800 °C a asymmetric for $\text{Ca}_{0.8}\text{Sr}_{0.2}\text{Ti}_{0.7}\text{Fe}_{0.3}\text{O}_{3-\alpha}$ membrane.¹⁰ The obtained results clearly indicate that mixing BFZ with LCC is quite effective for improving the oxygen permeability at medium and high temperature.

In order to know why the asymmetric LCC–BFZ membrane showed such high oxygen permeation, the activation energy of the oxygen permeation through the fabricated membranes was estimated. Inset of Figure 4 shows the Arrhenius plots of oxygen permeation fluxes. For the asymmetric LCC–BFZ membrane, the apparent activation energy was calculated from the slope of the plot to be 61.7 kJ mol^{-1} . The sintered-disk-type BFZ membrane shows the lowest apparent activation energy of 35.0 kJ mol^{-1} , while that of the sintered-disk-type LCC membrane was a largest value of 139.6 kJ mol^{-1} . The order of these values is well correlated with that of the lattice constants of the perovskite membranes, inferring that the expansion of the

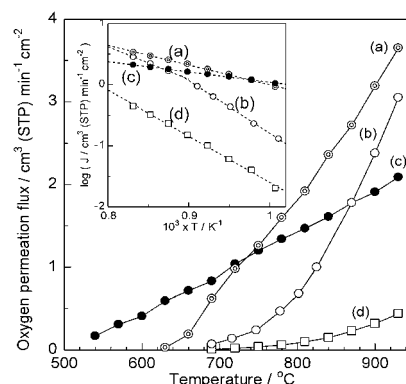


Figure 4. Oxygen permeation flux of asymmetric (a) LCC–BFZ (4:1) and (b) LCC membranes, and conventional sintered-disk-type (c) BFZ and (d) LCC membranes as a function of temperature. Inset shows the Arrhenius plots of the oxygen permeation fluxes above 700 °C.

lattice enhances the mobility of oxide ions and thus decreases the apparent activation energy. Such a relationship was also reported for other systems such as $\text{La}_{1-x}\text{Sr}_x\text{Fe}_{1-y}\text{Ga}_y\text{O}_3$.¹¹ Therefore, the increased oxygen permeability of the LCC–BFZ membrane is suggested to be due to the expansion of the lattice by formation of a solid solution of LCC and BFZ. However, the oxygen permeation flux of the asymmetric LCC–BFZ membrane was lower than that of the sintered-disk-type BFZ membrane (1000 μm) at around 650 °C. Thus, the fabrication of all BFZ-based dense/porous asymmetric structured membrane is highly desired for further improvement in the oxygen permeability at lower temperatures.

In conclusion, a thin dense LCC–BFZ (4:1 weight ratio) layer was successfully deposited on a porous LCC support to form a dense/porous asymmetric membrane. The fabricated asymmetric membrane showed high oxygen permeability at medium and high temperature such as 700–800 °C. It is suggested that the expansion of the lattice by formation of a solid solution of LCC and BFZ improved the mobility of oxide ions and increased the oxygen permeability.

This work was partially supported by CREST of JST (Japan Science and Technology Corporation), Steel Industry Foundation for the Advancement of Environmental Protection Technology, and Hosokawa Powder Technology Foundation.

References

- 1 Y. Teraoka, H. Zhang, S. Furukawa, N. Yamazoe, *Chem. Lett.* **1985**, 1743.
- 2 Y. Teraoka, T. Nobunaga, N. Yamazoe, *Chem. Lett.* **1988**, 503.
- 3 Z. Shao, G. Xiong, J. Tong, H. Dong, W. Yang, *Sep. Purif. Technol.* **2001**, 25, 419.
- 4 *Technical report for Development of Hydrogen-Manufacturing Technology from Steel-Making By-Product Gases*, The Japan Research and Development Center for Metals Foundation, Tokyo, **2006**.
- 5 Y. Teraoka, T. Fukuda, N. Miura, N. Yamazoe, *J. Ceram. Soc. Jpn. Inter. Ed.* **1987**, 97, 523.
- 6 K. Watanabe, M. Yuasa, T. Kida, K. Shimano, Y. Teraoka, N. Yamazoe, *Solid State Ionics* **2008**, 179, 1377.
- 7 D. Takauchi, K. Watanabe, K. Namidome, K. Shimano, Y. Teraoka, N. Yamazoe, Meeting of Electrochemical Society of Japan, Chiba, Japan, September, **2005**, Abstr. No. 2J33.
- 8 K. Watanabe, M. Yuasa, T. Kida, K. Shimano, Y. Teraoka, N. Yamazoe, *Chem. Mater.* **2008**, 20, 6965.
- 9 Y. Teraoka, H. Kakebayashi, I. Moriguchi, S. Kagawa, *Chem. Lett.* **1991**, 673.
- 10 S. Araki, Y. Hoshi, S. Hamakawa, S. Hikazudani, F. Mizukami, *Solid State Ionics* **2008**, 178, 1740.
- 11 V. V. Kharton, A. L. Shaulo, A. P. Viskup, M. Avdeev, A. A. Yaremchenko, M. V. Patrakeev, A. I. Kubakov, E. N. Naumovich, F. M. B. Marques, *Solid State Ionics* **2002**, 150, 229.